Enhancement in Mass Transfer Due to Motion of a Particle: An Experimental Study

The understanding of the mechanism of wall-to-bed heat and mass transfer in liquid-fluidized beds requires knowledge of the effect of the motion of individual particles on transfer processes. Experimental studies on the enhancement in mass transfer due to motion of a particle in the proximity of the transfer surface are presented. Mathematical relations based on a mechanistic model are obtained to describe the variation of the enhanced rate with time. The model parameters are correlated in terms of the particle Reynolds number, the wall-to-particle distance, and an interaction parameter that accounts for the background fluid motion. The results of this work would be of use in modeling transfer processes in other liquid-solid systems.

A. K. Verma, D. P. Rao
Department of Chemical Engineering
Indian Institute of Technology
Kanpur 208016, India

Introduction

It is known that particle convective transfer and fluid convective transfer are the two parallel modes of wall-to-bed heat transfer in fluidized beds. As the particle convective transfer is the dominant mode of heat transfer in gas-fluidized beds of smaller size particles, it has been extensively studied. It is recognized that the fluid convective transfer plays an equally important role in gas-fluidized beds of large particles such as fluidized bed combustors. In liquid-fluidized beds, the fluid convective transfer is the dominant mode of heat transfer, whereas it is the only mode in the case of mass transfer.

Only a few attempts have been made to understand the mechanism of fluid convective transfer. A brief summary of these attempts can be found in a paper by Adams (1982). In modeling the fluid convective transfer, the particles are assumed to be stationary and their influence on the thermal layer has been considered (Adams and Welty, 1979; Adams, 1982; Ganzha et al., 1982). A more realistic model should take account of the motion of particles. Such a model requires the velocity distribution of particles, voidage fluctuations, and enhancement in transfer processes due to individual particles. While there have been studies on the former two, the latter has received very little attention. Subramanian et al. (1973) have studied the effect of movement of a sphere in a thermal layer formed over a heated plate in still air. Valentine and Le Goff (1976) have examined the enhancement in mass transfer due to the impact of a particle on a transfer surface located on a cylinder placed perpendicular to the flow of liquid.

Exploratory studies, conducted to find the enhancement in transfer processes due to a sphere moving parallel to a plane wall, revealed that the enhancement at a location is larger and lasts longer in a liquid medium than in a gas medium. With a view to obtaining the detailed nature of the enhancement, mass transfer in a liquid medium was studied. In this paper, we present the studies on the enhanced mass transfer rate per unit length (along the axis of motion of particle) with time, with and without background fluid motion. The relevance of these studies has been demonstrated elsewhere (Verma, 1984) in modeling mass transfer in liquid-fluidized and packed beds. The studies would be of importance in understanding the transfer processes in other fluid-particle systems as well.

Experimental Method

Set-up

The well-known electrochemical technique of the reduction of potassium ferricyanide to potassium ferrocyanide in an excess inert electrolyte solution (Selman and Tobias, 1978) was employed for the measurement of mass transfer. The experimental set-up is shown in Figure 1. It consisted of an electrolytic bath (A), a particle mount (B), an x-y movement bench (C), and a support to hold the bench and the bath (D).

A 5 L beaker served as the electrolytic bath. A 6 mm thick Perspex sheet (E) 0.2 m × 0.12 m was fixed vertically in the beaker with an epoxy resin. The cathode (F), a nickel strip 18 mm × 3 mm, was fixed flush with the surface of the Perspex sheet. A nickel strip 0.25 m × 0.5 m was employed as the anode (G). The basis for arriving at the size of the cathode is discussed in the Appendix.

The half-T shaped particle mount, (B) in the elevation view of

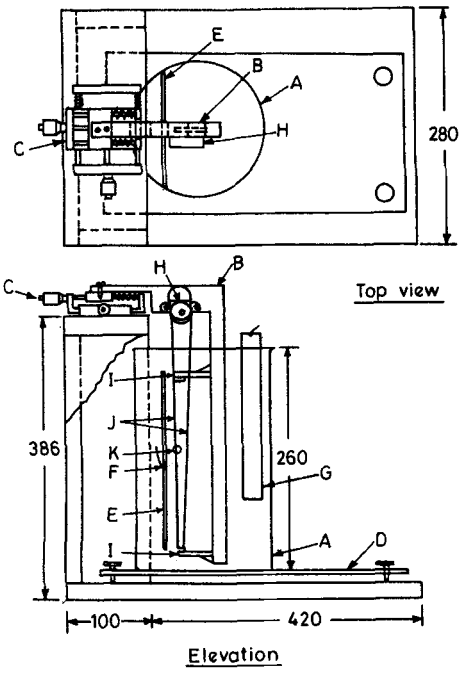

Figure 1. Experiment set-up.

A. Electrolytic bath
B. Particle mount
C. x-y movement bench
D. Support for bath and bench
E. Perspex sheet
F. Cathode
G. Anode
H. Motor
I. Arms
J. Nylon threads
K. Bead

Figure 1, was made of 0.6 mm thick Perspex sheet. A small motor (H), with a Perspex pulley, was fixed at the upper end of the particle-mount. Two arms (I), each with a pulley and a stainless steel guide wire, were attached to the stem of the particle mount. Two 0.05 mm dia. nylon threads (J), with a plastic bead (K), were looped over the motor and arm pulleys and were tied as shown in Figure 1. The motor (Hyden chart motor, 2.4 W, 220 V) had separate windings for clockwise and counterclockwise rotations. An up-and-down motion of the bead was achieved by switching the power from one winding to the other using an electronic timer circuit. Jerk-free motion of the bead was ensured by proper tension in the threads, and wobble-free motion by separating the threads by the stainless steel guide wires.

The distance between the bead and the cathode is an important variable. With the help of the x-y movement bench, the bead was positioned in front of the cathode. When seen from the side, the image of the bead was visible in the shining surface of the cathode. When the bead was touching the cathode, no separation between the bead and its image was visible. As the bead moved away, the point of separation was visible. The micrometer reading at which the separation just appeared was taken as the zero distance between the bead and the cathode, and it was measured with an accuracy of ±0.02 mm.

Procedure

An equimolar solution of potassium ferricyanide and potassium ferrocyanide of about 0.005 M each, with 1.0 M sodium hydroxide as an inert electrolyte, was used. Volumetric analysis was done to determine the ferricyanide concentration in the solution. For each run, which lasted about 6 h, fresh solution was used. Based on the preliminary measurements, a DC voltage of 0.5 V was applied across the cell to obtain the limiting current in all the runs. The limiting current was monitored using a data acquisition system (Hewlett-Packard model 3052A) as well as a strip chart recorder (Omega model O-5137-5M) in parallel.

After ensuring that the fluid was still in the beaker, the bead, which was positioned about 5 cm away from the cathode, was made to sweep past the cathode. It was stopped at about 8 cm from the cathode. In other cases, the bead was moved up and down about the cathode repeatedly. The sweep on either side of the cathode was controlled with the help of an electronic timer. Hereafter, the former motion of the bead is referred as "single sweep" and the latter as "multisweep." The limiting current, $i(t)$, was monitored from the start of the sweep until it attained nearly the still fluid value on stopping the bead.

Synchronous motors of different speeds as well as pulleys of different diameters were used to get various velocities of the bead. The bead velocity was checked and found to be uniform in all the cases. The temperature of the bath was monitored periodically. The physical properties of the solution were estimated as given by Eisenberg et al. (1956). The ranges of the relevant variables employed in this study are presented in Table 1. Further details can be found elsewhere (Verma 1984).

Enhancement in Mass Transfer: General Features

The mass transfer rate, $m(t)$, at a time t was computed from the well-known relation

$$m(t) = \frac{i(t)}{ZFc} \tag{1}$$

The variation of mass transfer rate with time due to a single sweep is shown in Figure 2 for a typical case. The inset at the right in the figure shows the relative positions of the particle (bead) and the cathode at different times. The $m(t)$ was constant before the particle arrived at point A, and its value corresponds to the still fluid condition. The mass transfer rate started increasing just after the arrival of the particle at the cathode. It may be noted that the rate increased only marginally by the time the wake (its length determined as given by Rimon and Cheng, 1969) had crossed the cathode, and it attained a maximum value much later. Minor periodic variations were observed in the

Table 1. Range of Variables Covered

Variable	Range
Particle dia., mm	3.01–5.84
Particle veloc., cm · s^{-1}	1.45–5.83
Reynolds no.	67.2–393.5
Solution viscosity × 10^{-3} kg · ms^{-1}	0.86–1.11
Solution density × 10^{-3} kg · m^{-3}	1.027–1.055
Diffusity × 10^{-12} m^2 · s^{-1}	7.2–8.9
Schmidt no.	970–1,060

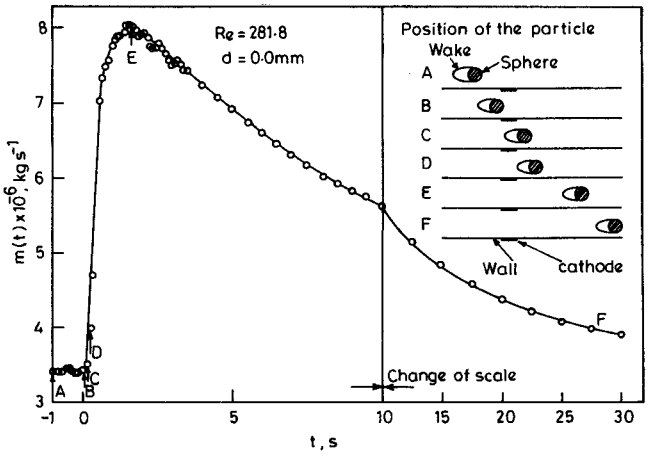

Figure 2. Variation of mass transfer rate with time, single sweep.

region of maximum rate for Reynolds numbers $Re > 110$. They became pronounced with increase in Re. (These fluctuations were recorded by the data acquisition system at a sampling rate of 10/s but the strip chart recorder gave only a smooth curve). These fluctuations could be attributed to vortex shedding by the wake. Weber and Bhaga (1982) found that the maximum liquid drift occurs at the point of maximum width of the bubble plus its combined wake. Hence, one would expect the maximum rate to occur about this point, but it was observed long after the wake had passed. This variance may be attributed to the proximity of the wall.

In general, it was observed that with the increase in the particle velocity or the particle diameter or with the decrease in the particle to wall distance, the maximum rate attained was higher, the time at which it occurred, t_m, was smaller, but the time taken to decay to the still fluid value was larger.

A typical variation of the mass transfer rate due to the multisweep is shown in Figure 3. The positions of the particle with respect to the cathode are shown in the inset at the lower left of the figure. It may be pointed out that only in the first sweep was the fluid still at the cathode when the particle arrived. In the

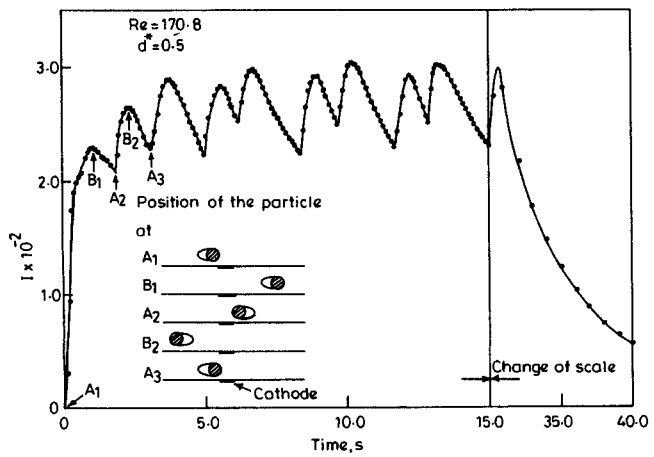

Figure 3. Variation of enhanced coefficient with time, multisweep.

subsequent sweeps, the fluid drift was in the opposite direction to the motion of the particle. This resulted in more intense fluid agitation that eventually attained a steady periodic nature. As a consequence, the mass transfer rate increased in the beginning and attained a steady periodic variation within six to seven sweeps. At the steady periodic variation, the maximum rates attained in the successive sweeps were different due to unequal sweep lengths set on either side of the cathode. When the particle was stopped, the rate decayed exponentially to the still fluid value. The periodic variations in the region of maximum rate were observed only in the first sweep, that too, when the time interval was large.

Mechanistic Model

The enhanced mass transfer rate can in principle be estimated if the flow field description is known. Such a fluid-mechanical description for the situation at hand is not available. In view of this, a mechanistic model is proposed with a limited objective of obtaining mathematical relations that could describe the variation of the enhanced rate with time for the single sweep and multisweeps.

As a sphere moves in an otherwise stagnant, unconfined fluid, the fluid elements close to the axis of motion are found to experience rather an abrupt outward radial velocity. They reverse their direction, and then drift in the direction of motion of the sphere (Weber and Bhaga, 1982). The proximity of the wall has an effect on the flow field, but the gross flow field is similar. Consider a volume, rectangular parallelpiped in shape, with the cathode as one of its sides and encompassing the flow field. In the case of single sweep, the time period from the time of arrival of the particle into the volume until the fluid became still, can be divided into two periods. The first of these can be viewed as a period of generation of kinetic energy in the volume. The second can be thought of as a period of decay in which the kinetic energy decays due to convection, dispersion, and viscous dissipation. In the case of multisweep, both the generation and decay of kinetic energy are affected by the background fluid agitation as well as the velocity of the particle.

Before proceeding with the model, it is convenient to introduce an "enhanced coefficient" $I_j(t)$, defined by the equation

$$I_j(t) = (m_j(t) - m_s)/Dwc \tag{1}$$

where j denotes the jth sweep after the particle has been set in motion, and t is the time elapsed since the time when the particle just arrived at the cathode in the jth sweep. The $I_j(t)$ is related to the local mass transfer coefficient as

$$I_j(t) = \frac{1}{D}\int_{-\infty}^{+\infty} [K_j(x, t) - K_s]\, dx \tag{2}$$

where $K_j(x, t)$ is the local mass transfer coefficient at a distance x from the axis of motion and K_s is the mass transfer coefficient at the still fluid condition. Since m_s, w, and c are invariants in a run, the nature of variation of $I_j(t)$ is similar to that of $m_j(t)$. For the sake of brevity, the enhanced coefficient is denoted by I_j.

Assuming that the I_j is a function of the kinetic energy of the fluid in the volume, the rate of change of I_j can be written as

$$\frac{dI_j}{dt} = G_j(t) + D_j(t) \tag{3}$$

where $G_j(t)$ and $D_j(t)$ are the rate of change of I_j due to the generation and decay of the kinetic energy, respectively.

As the first period lasts for only 5 s or less after the particle has crossed, the later part of I_j can be considered to be due to a pure decay. From the I_j vs. t curves for the single sweep and multisweep, it is found that the $D_j(t)$ can be represented by the simple relation

$$D_j(t) = -C_j I_j \tag{4}$$

For a number of cases, the $G_j(t)$ was deduced from the experimental I_j vs. t curves employing Eqs. 3 and 4. It was found that it can be represented by the empirical relation (Verma, 1984)

$$G_j(t) = a_j \exp\left(-\frac{b_j}{t} - C_j t\right) \tag{5}$$

Substituting Eqs. 4 and 5 in Eq. 3, it has been solved subject to the boundary condition

$$I_j = I_{jb} \quad \text{at} \quad t = 0$$

The constants a_j and b_j in the resulting equation have been eliminated using the conditions

$$I_j = I_{jm} \quad \text{at} \quad t = t_{jm} \tag{6a}$$

and

$$\frac{dI_j}{dt} = 0 \quad \text{at} \quad t = t_{jm} \tag{6b}$$

where t_{jm} is the time at which I_j attained its maximum value since the arrival of the particle at the cathode in the jth sweep. Thus, we obtain

$$I_j = \left(f I_{jm} \exp\left\{C_j t_{jm}\left[\frac{1 + f - (t_{jm}/t)}{f}\right]\right\} + I_{jb}\right) \exp(-C_j t) \tag{7}$$

where

$$f = 1 - \left(\frac{I_{jb}}{I_{jm}}\right) \exp(-C_j t_{jm})$$

For the single sweep, Eq. 7 reduces to a simple relation

$$I_1 = I_{1m} \exp\left[-C_1 (t_{1m} - t)^2 / t\right] \tag{8}$$

Model Verification

For the single sweep, the values of I_{1m} and t_{1m} were read from the I_1 vs. t curves, and the C_1 was evaluated from the data by regression analysis. Figure 4 shows the comparison of the estimated (using Eq. 8) and experimental I_1 vs. t curves. The agreement is good.

In the case of multisweep, I_{jb}, I_{jm}, t_{jm} were read from the I_j vs. t curves and the values of C_j were evaluated from the jth sweep data. Figure 5 shows comparison of the experimental and estimated I vs. t curves for a few cases. The agreement is good except at larger times where I_j approached the still values. It

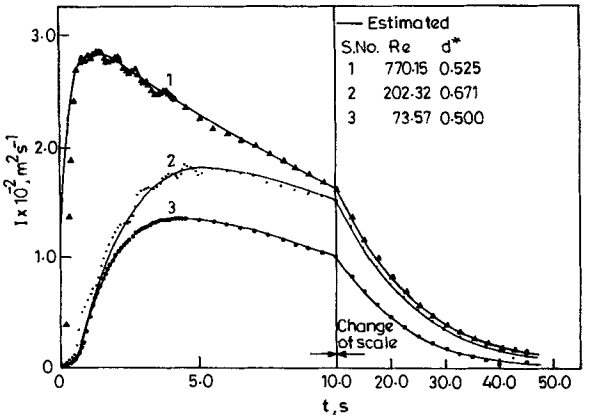

Figure 4. Variation of experimental and estimated (Eq. 8) enhanced coefficients with time, single sweep.

appears that Eqs. 7 and 8 describe adequately the variation of the enhanced coefficient.

Correlation of Model Parameters

Single sweep

The correlations of the model parameters for the single sweep, along with the ranges, are given below

$$I_{1m} = 5.98(d^*)^{-1.11} Re^{0.56} \tag{9}$$

$$t^*_{1m} = 28.1(d^*)^{1.81} Re^{0.12} \tag{10}$$

$$C_1 = 0.62(d^*)^{0.17} Re^{-0.38} \tag{11}$$

$$60 < Re < 395, \; 0.5 < d^* < 1.1$$

where

$$t^*_{1m} = \frac{t_{1m} V_p}{dp}, \quad d^* = \frac{d + \frac{d_p}{2}}{d_p}$$

The enhanced coefficients estimated from the correlations are

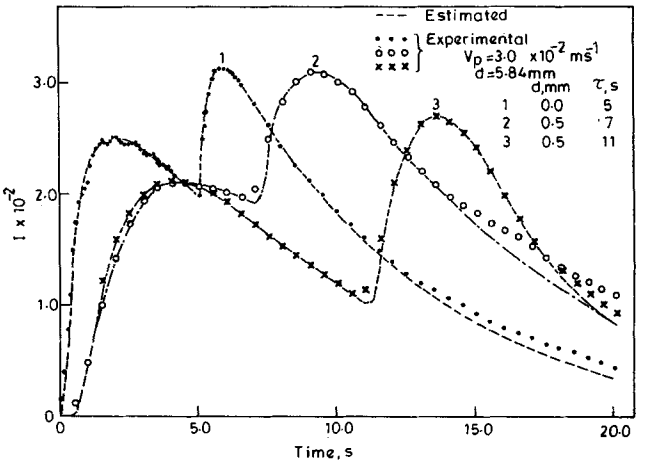

Figure 5. Variation of experimental and estimated (Eq. 7) enhanced coefficients with time, multisweep.

compared with the experimental data in Figure 6 for a few cases. In this figure, the data points are omitted for the sake of clarity. The average deviation between the estimated and experimental values is 20%, and 95% of the data are within 35%.

Multisweep

To correlate the multisweep data, it was considered that an additional parameter is needed to account for the effect of the background fluid motion on the enhanced coefficient. Of the several possible interaction parameters tried, I_{jb}/d_p was found to give a better fit of the data. The correlations obtained along with their ranges of validity are presented below.

$$\ln\left(\frac{I_{jm}-I_{jb}}{I_{1m}}\right) = -3.06\times10^{-4}(d^*)^{1.58}Re^{-0.35}\left(\frac{I_{jb}}{d_p}\right) \quad (12)$$

$$\ln\left(\frac{t_{jm}}{t_{1m}}\right) = -3.31\times10^{-3}(d^*)^{1.1}Re^{-0.75}\left(\frac{I_{jb}}{d_p}\right) \quad (13)$$

$$\ln\left(\frac{C_j}{C_1}\right) = 1.94\times10^{-3}(d^*)^{0.17}(Re)^{-0.86}\left(\frac{I_{jb}}{d_p}\right) \quad (14)$$

$$90<Re<395, 0.5<d^*<0.84, 3.18\times10^4<\frac{I_{jb}}{d_p}<1.28\times10^5$$

The enhanced coefficient for the multisweeps was estimated as follows. Using the correlations for the single sweep, the I_1 with t was evaluated until the time of arrival of the particle, t_1, for the next sweep. Setting I_1 at t_1 to I_{2b}, the I_2 with t was found from Eqs. 7 to 14. Likewise, I_j vs. t was found for the subsequent sweeps. The comparison of experimental and estimated values is shown in Figure 7. In general, the deviations are considerable in the first few sweeps and more so at larger wall-to-particle distance, but the agreement is better at the steady periodic conditions.

To assess the overall accuracy of the correlations, the average values of experimental and estimated I_j were computed from the

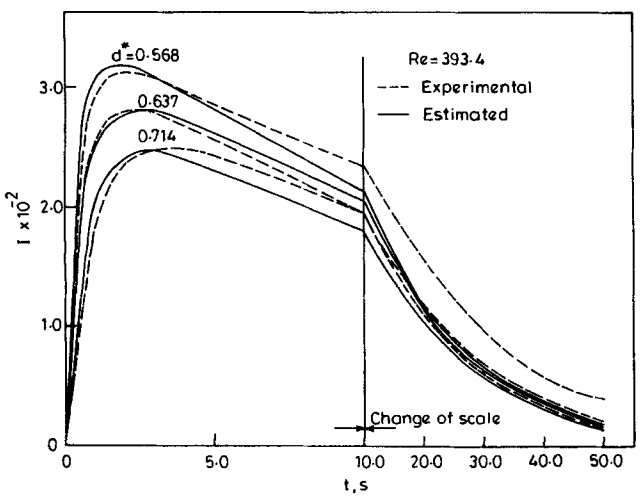

Figure 6. Experimental and estimated (from correlations) enhanced coefficients, single sweep.

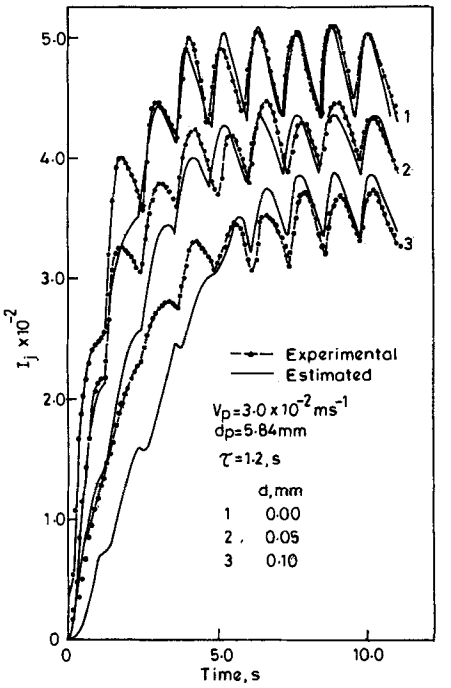

Figure 7. Experimental and estimated (from correlations) enhanced coefficients, multisweep.

equation

$$I_{av} = \frac{1}{\sum_{j=1}^{n} t_j}\sum_{j=1}^{n}\int_0^{t_j} I_j\,dt$$

and are compared in Figure 8. The average deviation is 19%, and 80% of the data are within 25% deviation.

Conclusions

The enhancement in mass transfer rate, from a strip electrode, due to a single sweep and due to repeated up-and-down

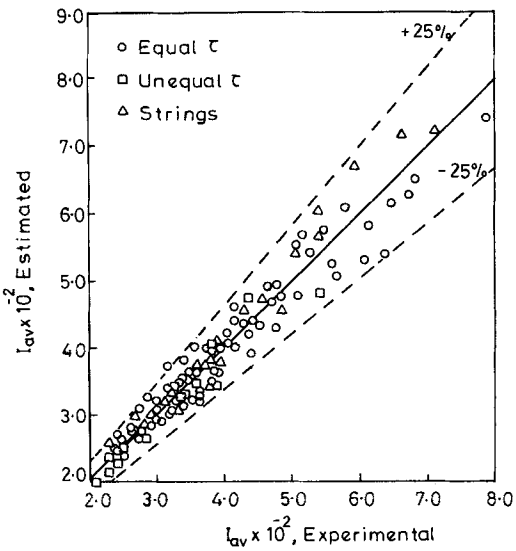

Figure 8. Experimental and estimated average enhanced coefficients.

motion of a particle has been studied. Mathematical relations based on a mechanistic model have been obtained to describe the variation of the rate with time. An interaction parameter has been identified to account for the effect of background flow field on the enhanced rate. Empirical correlations are proposed for the estimation of the enhanced rate due to the particle motion. The results of this study would be of use in modeling the transfer processes in liquid-solid systems.

Notation

a = constant, Eq. 5
b = constant, Eq. 5
c = concentration of potassium ferricyanide, kmol · m^{-3}
C = decay constant, Eq. 4
d = wall-to-bead distance, m
d_p = diameter of particle, m
D = diffusivity of reacting ion, $m^2 \cdot s^{-2}$
$D(t)$ = rate of change of I due to decay of kinetic energy at time t
f = defined by Eq. 7
F = Faraday's constant
$G(t)$ = rate of change of I due to generation of kinetic energy at time t
$i(t)$ = limiting current at time t, A
$I, I(t)$ = enhanced coefficient, Eq. 1
$K, K(x, t)$ = local mass transfer coefficient at x and t, m · s^{-1}
L = length of cathode, m
$m, m(t)$ = mass transfer rate at time t, kmol · s^{-1}
n = number of sweeps
Re = Reynolds number
t = time, s
w = width of cathode, m
x = distance from center of cathode, m
Z = valence charge of an ion, kg · Aeq · $kmol^{-1}$

Subscripts

av = average
b = value at $t = 0$
j = jth sweep
m = maximum
s = value at still fluid condition
1 = first sweep

Superscript

* = dimensionless quantities, Eqs. 9, 11

Appendix: Cathode Size

This section describes how the dimensions of the cathode were fixed. Motion of the bead with respect to the cathode is shown in Figure A1a. As the particle sweeps past the cathode in an otherwise still fluid, the instantaneous local mass transfer coefficient $K(x, t)$ is expected to vary with x as shown in Figure A1b.

Soon after the bead has crossed the cathode, the flow field along the cathode is characterized by reversing and unsteady flows at the center of the cathode. Away from the center it is unsteady laminar flow, and beyond that the fluid is nearly still. Only at large times does the flow at the center becomes laminar as the agitation dies down. The expected variation of $K(x, t)$ is shown in Figure A1b. The area under the bell-shaped curve gives the enhanced coefficient. The smaller the width of the cathode, the larger are the edge effects due to three-dimensional diffusion. On the other hand, as the width is larger, the variation of $K(x, t)$ along the width of the cathode is larger. In this study, the time taken by the particle to cross over a cathode of 3 mm width was in the range of 0.035 to 0.35 s. In this time interval,

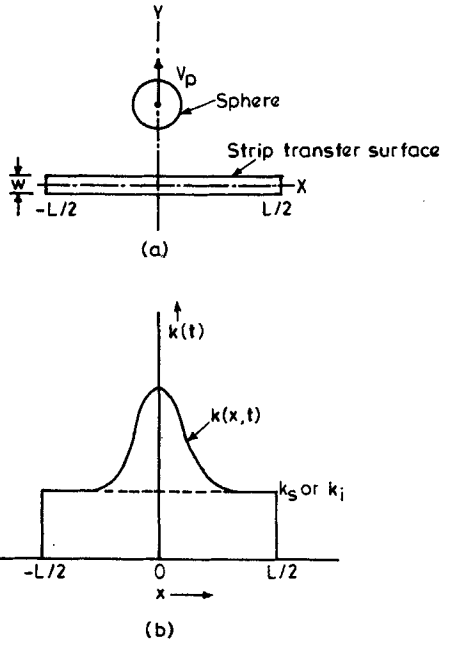

Figure A1. Configuration of cathode and bead. (b) Variation of local mass transfer coefficient along length of cathode.

the variation of the enhanced mass transfer rate was found to be negligible except for a very brief initial period. Hence, the diffusional layer is assumed to be uniform along the width in view of the reversing and turbulent flow field, and high Schmidt number (>1,000). As the thickness of the diffusional layer is of an order of magnitude smaller than 3 mm, the edge effects are expected to be negligible. Hence, a cathode of 3 mm width was considered adequate for the measurement of the local enhanced coefficient.

To decide on the length of the cathode, the local mass transfer coefficients were measured as described below. The axis of motion of the particle was shifted to one of the edges of the cathode and the enhancement in mass transfer was monitored. Then, the axis of motion was shifted away from the cathode by about 0.5 mm (Δx) and again the mass transfer rate was monitored.

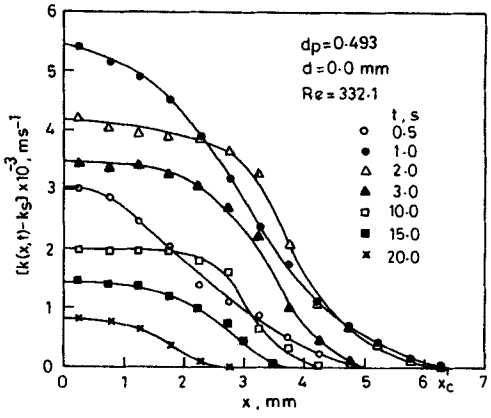

Figure A2. Variation of local mass transfer coefficient with distance from center of cathode.

From the difference of these rates, the $K[x + (\Delta x/2), t]$ was computed. Shifting the axis of motion by appropriate increments, the $K(x, t)$ were obtained until they remained constant. A typical set of $K(x, t)$ is given in Figure A2. For the extreme case encountered, the x_c was found to be 6.5 mm and hence a cathode of 18 mm length was employed.

Literature Cited

Adams, R. L., "Coupled Gas Convection and Unsteady Conduction Effects in Fluid Bed Heat Transfer Based on a Single-Particle Model," *Int. J. Heat Mass Trans.*, **25**, 1819 (1982).

Adams, R. L., and J. R. Welty, "A Gas Convection Model of Heat Transfer in Larger Particle Fluidized Beds," *AIChE J.*, **25**, 395 (1979).

Eisenberg, M., C. W. Tobias, and Wilke, "Selected Physical Properties of Ternary Electrolytes Employed in Ionic Mass Transfer Studies," *J. Electrochem. Soc.*, **103**, 413 (1956).

Ganzha, V. L., S. N. Upadhyay, and S. C. Saxena, "A Mechanistic Theory for Heat Transfer between Fluidized Beds of Large Particles and Immersed Surfaces," *Int. J. Heat Mass Trans.*, **25**, 1534 (1982).

Rimon, Y., and S. I. Cheng, "Numerical Solution of a Uniform Flow over a Sphere at Intermediate Reynolds Number," *Phys. Fluids*, **12**(5), 949 (1969).

Selman, J. R., and C. W. Tobias, "Mass Transfer Measurements by the Limiting Current Technique," *Advances in Chemical Engineering*, **10**, Academic Press, New York, 211 (1978).

Subramanian, N., D. P. Rao, and T. Gopichand, "Effect on Heat Transfer due to a Particle in Motion through Thermal Boundary Layer over a Flat Plate," *Ind. Eng. Chem. Fundam.*, **12**, 479 (1973).

Valentine, G., and P. Le Goff, "Fluidization Par Liquid: Etude du Transfer de Matiere Entre le Liquid et un Object Mobile Dans le Lit," *Lett. Heat Mass Trans.*, **6**, 157 (1979).

Verma, A. K., "Studies on the Mechanism of Wall-to-Bed Mass Transfer in Liquid-Fluidized Beds: A Single-Particle Approach," Ph.D., Thesis, Indian Institute of Technology, Kanpur, India (1984).

Weber, M. E., and D. Bhaga, "Fluid Drift Caused by a Rising Bubble," *Chem. Eng. Sci.*, **37**, 113 (1982).

Manuscript received Aug. 23, 1984, and revision received Feb. 12, 1988.